



UNIVERSITÀ POLITECNICA DELLE MARCHE  
Repository ISTITUZIONALE

Long term correlation and inhomogeneity of the inverted pendulum sway time-series under the intermittent control paradigm

This is the peer reviewed version of the following article:

*Original*

Long term correlation and inhomogeneity of the inverted pendulum sway time-series under the intermittent control paradigm / Tigrini, A.; Verdini, F.; Fioretti, S.; Mengarelli, A.. - In: COMMUNICATIONS IN NONLINEAR SCIENCE & NUMERICAL SIMULATION. - ISSN 1007-5704. - STAMPA. - 108:(2022). [10.1016/j.cnsns.2021.106198]

*Availability:*

This version is available at: 11566/294354 since: 2024-04-25T09:56:25Z

*Publisher:*

*Published*

DOI:10.1016/j.cnsns.2021.106198

*Terms of use:*

The terms and conditions for the reuse of this version of the manuscript are specified in the publishing policy. The use of copyrighted works requires the consent of the rights' holder (author or publisher). Works made available under a Creative Commons license or a Publisher's custom-made license can be used according to the terms and conditions contained therein. See editor's website for further information and terms and conditions.

This item was downloaded from IRIS Università Politecnica delle Marche (<https://iris.univpm.it>). When citing, please refer to the published version.

note finali coverage

(Article begins on next page)

# Long Term Correlation and Inhomogeneity of the Inverted Pendulum Sway Time-Series under the Intermittent Control Paradigm

Andrea Tigrini<sup>a</sup>, Federica Verdini<sup>a</sup>, Sandro Fioretti<sup>a</sup>, Alessandro Mengarelli<sup>a,\*</sup>

<sup>a</sup>*Department of Information Engineering, Università Politecnica delle Marche, 60131, Ancona, Italy*

---

## Abstract

In this study the extended detrended fluctuation analysis (EDFA) was applied to the sway data generated from an inverted pendulum (IP) model, intermittently controlled at the ankle. The time series taken into account was the center of pressure (COP), since it represents the widest used time series in posturography, and it constitutes a natural link between model and data-based analysis approaches for studying the dynamics of the human balance maintenance. COP time-series were obtained by varying the intermittent control parameters (ICP) in a uniform distribution range that ensures IP stability to quantify changes in the long-term correlation and inhomogeneity of the time-series. Globally, EDFA coefficients ( $\alpha$  and  $\beta$ ) showed to be sensitive to the variations of derivative control gain ( $D$ ), whereas for proportional gain ( $P$ ) and  $\rho$  parameters no significant trends were observed. However, relations between EDFA coefficients and  $\rho$  arose whether derivative gain is examined within a low and high regions of value. For low  $D$  gains, both  $\alpha$  and  $\beta$  showed a significant correlation with  $\rho$ , which disappears when higher  $D$  values were considered. Thus EDFA coefficients can provide useful insights about the long-term correlation and local characteristics of COP timeseries, which are strictly related to the control policy adopted

---

\*Fully documented templates are available in the elsarticle package on CTAN.

\*Corresponding author

*Email addresses:* [a.tigrini@pm.univpm.it](mailto:a.tigrini@pm.univpm.it) (Andrea Tigrini), [f.verdini@staff.univpm.it](mailto:f.verdini@staff.univpm.it) (Federica Verdini), [s.fioretti@staff.univpm.it](mailto:s.fioretti@staff.univpm.it) (Sandro Fioretti), [a.mengarelli@pm.univpm.it](mailto:a.mengarelli@pm.univpm.it) (Alessandro Mengarelli)

for maintaining balance. This supports the validity of the intermittent motor control paradigm for the human upright stance and suggests the use of EDFA in real posturography applications, in order to extract meaningful information regarding the properties of COP timeseries for different groups of patients.

*Keywords:* Center of Pressure (COP), Intermittent control, Extended detrended fluctuation analysis (EDFA)

---

## 1. Introduction

The study of bipedal upright stance and balance maintenance has fascinated many different scientific disciplines. Indeed, understanding the hidden mechanisms that the central nervous system (CNS) employs to control the body mechanics is fundamental in neurorobotics to embody intelligence in humanoid robots [1, 2], but even in neuroscience and posturography, to better understand how pathologies affecting CNS may impact on the motor control [3, 4]. In this scenario, approaches that combine biomechanical modeling of the stance and the analysis of time-series, such as the evolution of the center of mass (COM) and the center of pressure (COP) [5, 6, 7], grounded the bases for a deeper comprehension of the motor control policies actuated by the CNS.

Although stiffness-based stabilizing mechanisms and continuous control paradigm are widely used in literature to model the neuromuscular control of stance [8, 9], the intermittent control approach demonstrated to be supported by physiological evidence [10]. As first, muscle activity is bursting, and it may be mirrored in the control torques at the human joints [6]. Furthermore, Morasso, Schieppati, and Sanguineti [11, 12] highlighted the inability of the ankle stiffness alone to compensate the whole body gravity pull, without an active mechanism played by the CNS [5]. Moreover, the intermittent control policy can generalize a continuous one, as highlighted in [7]. Thus, despite the real motor control paradigm of the stance maintenance is unknown, it is plausible that the CNS can take advantage from the body structure in order to develop a control strategy that does not act continuously [10]. Indeed, global stability of the system can be

24 obtained switching between unstable dynamics [10, 13], hence through a variable  
25 structure control policy. The idea of intermittency, meant as an agent that acts  
26 when necessary, was hypothesized also by Collins and De Luca [14], following  
27 a time-series analysis approach, i.e. the stabilogram diffusion analysis (SDA)  
28 [14].

29 Despite the two previous perspectives, i.e. model-based and time-series anal-  
30 ysis, are different [7], the need for a unified perspective results of great impor-  
31 tance when one would obtain highly explainable models. Indeed, in [7] the  
32 aforementioned approaches were combined through the approximate bayesian  
33 computation, in order to infer the parameters of the intermittent controller  
34 from posturographic data. This makes more underpinned the interpretation  
35 of the results if compared to models obtained through black box identification  
36 procedures, where high fidelity data fitting could be paid with a limited inter-  
37 pretability. Literature shows other studies that followed the inclusive approach  
38 stated above. In [15] for instance, SDA was applied to simulated COP data  
39 obtained by using a simple inverted pendulum (IP) model, commonly used to  
40 describe the mechanics of the body stance, varying the continuous controller  
41 parameters, and then examining their relation with the SDA coefficients [14].  
42 Also in [10], changes in the intermittent control parameters (ICP) were related  
43 to changes in the power spectral density (PSD) of the sway data. Furthermore,  
44 such PSDs reproduced the multiple law scaling properties observed in data ac-  
45 quired during human quiet stance [10].

46 The investigation of intermittent control models of human stance through  
47 time series analysis approaches is far to be completely assessed. In particular,  
48 as emerged from previous works [15, 16, 6, 17], a possible way to carry on  
49 such investigation is to employ COP model-generated data. This for two main  
50 reasons: firstly, the COP can be directly measured from force platforms without  
51 the need for any motion capture systems, commonly used to estimate the COM.  
52 Thus, the knowledge extracted from the model can be validated through real  
53 data. Secondly, COP is directly related with the control torques generated at  
54 the ankle and upper joints of the body [11, 8, 14], and hence it contains the

55 sign of the CNS control action. Another important aspect regards the selection  
56 of adequate descriptors used to evaluate the COP time-series. In [18] different  
57 spatial, temporal and frequency COP descriptors were presented. However, they  
58 do not account for the nonlinear properties and long-term correlation of COP  
59 data. Instead, other authors approached the study of COP time-series through  
60 the use of SDA, rambling and trembling decomposition, sway density curve and  
61 detrended fluctuation analysis (DFA) [14, 19, 4, 20, 21]. These are only few of  
62 the methodologies employed to capture more detailed information regarding the  
63 nature of biological processes behind balance maintenance.

64 Recently, an extension of the DFA, named extended DFA (EDFA), was pro-  
65 posed in [22]. EDFA grounds its basis on the fact that experimental data often  
66 present inhomogeneity due to changes in the dynamics of the systems. This  
67 aspect can be encountered in many biological time series, ranging from heart  
68 rate to electroencephalography [23, 24]. Moreover, behind EDFA there is the  
69 idea to quantify not only the slow variations in the local mean value, as done  
70 by DFA, but also to consider other types of non-stationary behaviors, such as  
71 those induced by intermittency or faster oscillations [23]. Thus in this study,  
72 EDFA was applied to simulated COP time course obtained through intermit-  
73 tent control paradigm, applied to an IP model, and by varying the ICP within  
74 a plausible range [10, 7]. Then, EDFA coefficients were computed to asses how  
75 changes in the ICP affect posturographic data, and if EDFA can highlight hid-  
76 den properties of the motor control paradigm employed to stabilize the IP.

77 The paper is organized as follows. Methods section describes the human  
78 stance model based on the intermittent controller used to generate simulated  
79 COP, then EDFA principles are recalled. Results are thus presented and dis-  
80 cussed in the third section, and concluding remarks reported in the last section  
81 end the paper.

82 **2. Materials and Methods**

83 *2.1. Upright stance balance maintenance model and data generation*

84 The human balance maintenance model considered in this study was pre-  
 85 sented in [10], and it basically develops a variable structure control system to  
 86 describe the body sway in quiet conditions. The latter can be modeled through  
 87 an IP linearized in the neighborhood of the vertical equilibrium point [10]. Thus,  
 88 the dynamics is given by:

$$I\ddot{\theta} = mgh\theta - T \quad (1)$$

89 where  $\theta$  is the COM sway angle in the sagittal plane,  $m$  is the subject body  
 90 mass,  $h$  is the distance of the COM with respect to the ankle,  $g$  is the gravity  
 91 acceleration, and  $I$  is the moment of inertia of the body around the ankle. The  
 92 term  $mgh\theta$ , hence represents the gravitational toppling torque that is dynam-  
 93 ically counterbalanced by  $T$ , i.e. the control torque applied at the pendulum  
 94 joint. The latter can be modeled as in [10, 6]:

$$T = K\theta + B\dot{\theta} + f_P(\theta_\Delta) + f_D(\dot{\theta}_\Delta) + \sigma\xi \quad (2)$$

95 The first two terms ( $K\theta$  and  $B\dot{\theta}$ ) model the passive feedback torques due to  
 96 ligament and muscle tone. On the contrary,  $f_P(\theta_\Delta)$  and  $f_D(\dot{\theta}_\Delta)$  model the  
 97 active role played by the CNS that has been thought intermittent, depending  
 98 on the portion of the phase plane the state is at a given time [10]. To be  
 99 noted, the two terms depend respectively to the delayed sway angle and its  
 100 time derivative. Indeed  $\theta_\Delta = \theta(t - \Delta)$ , where  $\Delta$  represents the physiological  
 101 neural delay that accounts for both the afferent and efferent neural information  
 102 transmission [10]. The last term in the right hand side of (2) represents the  
 103 internal postural noise, modeled as an additive Gaussian white noise  $\xi(t)$  with  
 104 standard deviation  $\sigma$  [10].

105 The switching policy adopted for the model was defined in [10] and used also  
 106 in [6]. It can be summarized as follows:

$$\begin{cases} f_P(\theta_\Delta) = P\theta_\Delta; & f_D(\dot{\theta}_\Delta) = D\dot{\theta}_\Delta; & \text{if } \theta_\Delta(\dot{\theta}_\Delta - l\theta_\Delta) > 0 \\ f_P(\theta_\Delta) = 0; & f_D(\dot{\theta}_\Delta) = 0; & \text{otherwise} \end{cases} \quad (3)$$

107 where  $P$  and  $D$  represents the proportional and derivative gains of the active  
 108 controller, while  $l$  characterizes the slope of the on-off boundary lines  $\dot{\theta}_\Delta = l\theta_\Delta$   
 109 [10, 7]. As highlighted in [7], for the closed loop system described above, the  
 110 switching activity is driven by the portion of the phase plane where the active  
 111 controller is turned on with respect to the whole phase plane (Fig. 1). This  
 112 quantity can be defined as  $\rho$  and it is formally equivalent to [7]:

$$\rho = \frac{S_{on}}{S_{on} + S_{off}} \equiv 0.5 - \frac{\arctan(l)}{\pi} \quad (4)$$

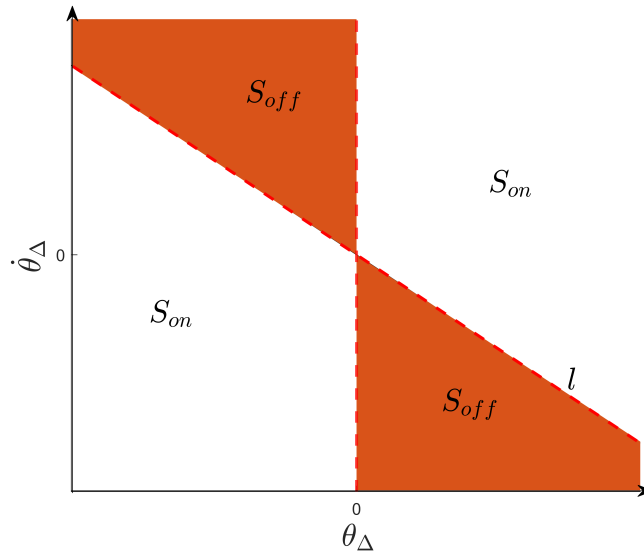


Figure 1: Schematic representation of the phase space portion in which the active controller is turned on ( $S_{on}$ ) and off ( $S_{off}$ ). The two regions were determined by the switching condition in equation (3) where  $l$  determines the on-off boundary region.

113 To be noted, if the active controller is continuously turned on, the  $S_{off}$  area is  
 114 equal to zero ( $\rho = 1$ ), and the model generalizes the continuous motor control  
 115 paradigm [15, 7]. For a non-null  $S_{off}$  the active controller is turned on and off  
 116 ( $\rho < 1$ ) and the motor control paradigm is the intermittent one. Eventually,  
 117 if the  $S_{on}$  area is zero ( $\rho = 0$ ), the active controller never turns on and the  
 118 pendulum stabilization can be reached only through the passive components of  
 119  $T$ .

120 However, as reported in [12], ankle stiffness alone cannot stabilize the upright  
121 stance, and by following the line proposed in [10], the stiffness term  $K$  (see  
122 equation (2)) was set at the 80% of  $mgh$ . In this way, an active control is  
123 always required [7, 11]. To run the simulations, the model parameters and the  
124 ICP, i.e.  $(P, D, \rho)$ , were set as reported in table 1. The forward Euler method  
125 with a time step of 0.001 s was used to solve the delayed differential equation  
126 given by (1) after substitution of  $T$  through (2). Further details regarding the  
127 discretization and integration procedures can be found in [10, 7].

128 One thousand stable simulations of 60 s were run sampling  $(P, D, \rho)$  from  
129 opportune uniform distributions (Table 1). For each simulation, the COP with  
130 respect to the ankle joint was obtained following the relation [25]:

$$COP = COM - \frac{h}{g}C\ddot{O}M \quad (5)$$

131 where  $COM$  can be obtained by the sway data since is the projection of the cen-  
132 ter of mass in the anterior posterior direction. More precisely, COM is obtained  
as  $COM = h \sin(\theta)$ .

Table 1: Table shows the model parameters and the ICP used to simulate the model.  $P$ ,  $D$   
and  $\rho$  were sampled from uniform distributions in plausible ranges [6, 7, 13]

$m$	$I$	$h$	$B$	$K$	$g$	$\Delta$	$\sigma$	$P$	$D$	$\rho$
(kg)	(kg·m <sup>2</sup> )	(m)	(N·m·s/rad)	(N·m/rad)	(m/s <sup>2</sup> )	(s)	(N·m)	(N·m/rad)	(N·m·s/rad)	
60	60	1	4.0	471	9.81	0.2	0.2	$\mathcal{U}_{[294; 471]}$	$\mathcal{U}_{[0; 400]}$	$\mathcal{U}_{[0.3; 1]}$

133

## 134 2.2. Extended detrended fluctuation analysis

135 Given a time series  $x(i)$  of length  $N$ , the DFA involves the transformation  
136 of  $x(i)$  in its profile  $y(i)$  through an integration after mean removal [26, 24]:

$$y(k) = \sum_{i=1}^k [x(i) - \langle x \rangle], \quad \langle x \rangle = \frac{1}{N} \sum_{i=1}^N x(i) \quad (6)$$

137 The resulting profile or random walk undergoes to non-overlapping segmenta-  
138 tions of equal length  $n$ . Then, for each segment of the profile, a local trend



139  $y_n(k)$  is computed through a linear fit in a least square sense [23]. When local  
 140 trend is available, one can proceed by computing the fluctuation, or standard  
 141 deviation of the signal profile around the local trend as:

$$F(n) = \sqrt{\frac{1}{N} \sum_{k=1}^N [y(k) - y_n(k)]^2} \quad (7)$$

142 The process is iterated for different segment size ( $n$ ) in order to obtain  $F(n)$   
 143 over a possible large number of scales. In general,  $F(n)$  presents a power law  
 144 behavior of the type:

$$F(n) \sim n^\alpha \quad (8)$$

145 where the  $\alpha$ -exponent can be estimated through the log-log representation of  
 146  $F(n)$  versus  $n$  [24, 26].

147 What reported until now are the basic steps of the DFA. However, as high-  
 148 lighted in [23], the inhomogeneity of the data, which can be due to multiple  
 149 dynamics interactions, can lead to a consistent variability of the profile fluctu-  
 150 ations around the local trend among the different signal epoch sizes ( $n$ ). This  
 151 can produce a departure from model (8), rendering more challenging the inter-  
 152 pretation of the classical DFA. To mitigate this aspect, in [22, 23] the authors  
 153 proposed a DFA extension, namely EDFA, that takes care of the heterogeneity  
 154 in the RMS fluctuations. Hence, in addition to the canonical DFA, one can  
 155 consider the following quantity:

$$dF(n) = \max[F_{loc}(n)] - \min[F_{loc}(n)] \quad (9)$$

156 where  $dF(n)$  is the difference between the maximum and minimum local RMS  
 157 fluctuations  $F_{loc}(n)$  [23]. Here, the local RMS fluctuations of the signal profile  
 158  $y(k)$  from the trend  $y_n(k)$  depends on the epoch length ( $n$ ). As observed in  
 159 [23], also  $dF(n)$  could change with  $n$ , following a power-law dependence with  
 160 another scaling exponent  $\beta$ :

$$dF(n) \sim n^\beta \quad (10)$$

161 The EDFA was applied to each COP trace generated as described in section  
 162 2.1, and both  $\alpha$  and  $\beta$  were computed to evaluate how changes in the ICP

163 impact on the simulated COP time-series.

### 164 **3. Results and Discussion**

165 In Figure 2 the mean trends among all the simulated time series of both  
166  $F$  and  $dF$  are shown in the log-log scale. A greater variability is present at  
167 higher time scales and an inverse relation exists between ( $n$ ) and the frequency,  
168 as underlined in [27]:

$$n(f) = \frac{f_s}{f} \quad (11)$$

169 where  $f_s$  is the sampling frequency and  $f$  is the considered frequency. This  
170 suggests that modifications of the active controller parameters lead to changes  
171 of balance response focused at the higher time scales and thus at the lower  
172 frequency ranges [10], aligning with [28], where the effects of neural control on  
173 COP data were observed in the lower bands (LB) frequency range of 0.5-0.1  
174 Hz. Confirmations can be found also in [27], where part of such neural feedback  
175 due to the visuo-vestibular information should be mirrored in COP time-series  
176 at frequencies lower than 0.5 Hz [27]. This aspect supports the goodness of  
177 the intermittent motor control paradigm, since modifications of its parameters  
178 produce larger variations at the LB ranges (Fig. 3), thus in according with the  
179 regulatory activity of the CNS in the human balance maintenance, focused on  
180 the frequency LB [28, 10, 27]. For the above mentioned reasons, one can focus  
181 on the fluctuations at the higher time scales to observe the behavior of both  $F$   
182 and  $dF$  in the LB.

183 The EDFA appears suitable for capturing variations in the active control  
184 policy: observing the  $F$  and  $dF$  fluctuations restricted at the LB (Fig. 3), one  
185 can appreciate that both type of fluctuations are affected by ICP variations and  
186  $dF$  showed a greater level of variability at all the ( $n$ ) with respect to  $F$ , likely  
187 indicating that  $dF$  responds to the same control parameters changes by greater  
188 modifications of its value (Fig. 3).

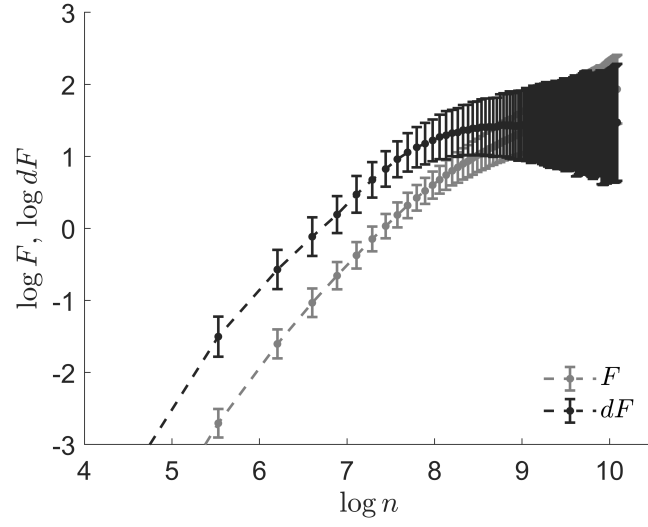


Figure 2: Log-log representation of the EDFA fluctuations in mean and standard deviation, the latter were computed over the 1000 synthetic COP time-series generated by the model.

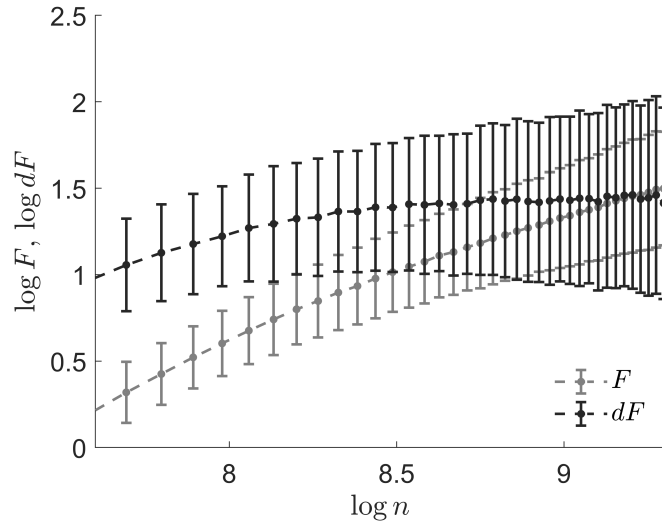


Figure 3: Log-log representation of the EDFA fluctuations in mean and standard deviation. Focus on the time scales that maps the frequency band 0.5-0.1 Hz.

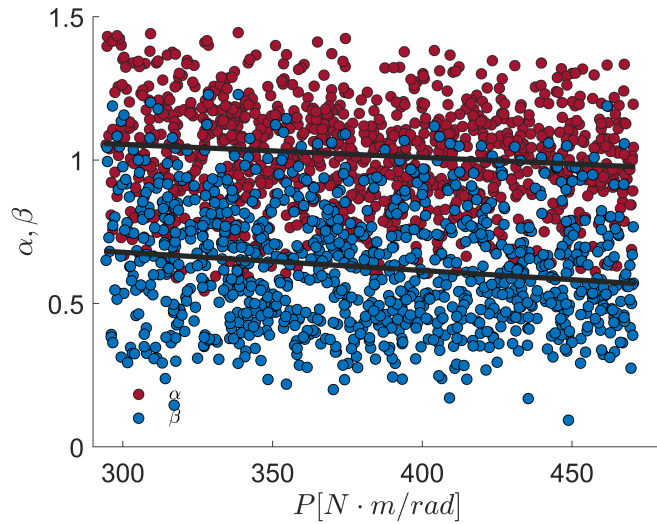


Figure 4: EDFA coefficients  $\alpha$  and  $\beta$  obtained for the simulated COP time series and scattered in relation to  $P$  parameter. The correlation coefficients results  $r = -0.12$  and  $-0.15$ , for  $\alpha$  and  $\beta$  respectively. Figure shows also the linear trend between  $P$  and the coefficients.

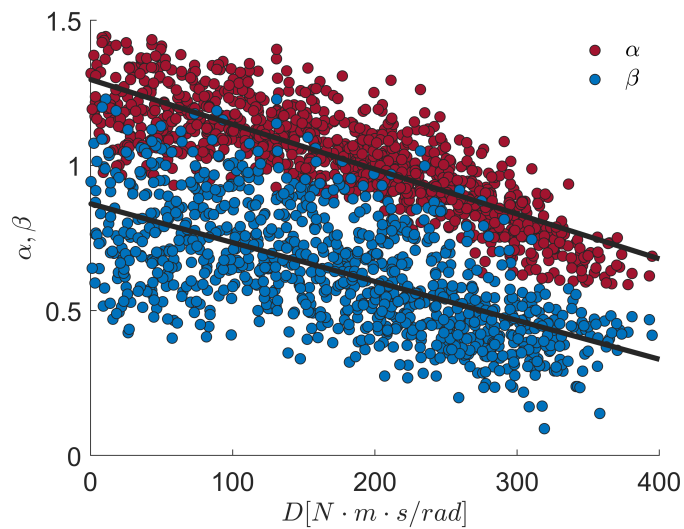


Figure 5: EDFA coefficients  $\alpha$  and  $\beta$  obtained for the simulated COP time series and scattered in relation to  $D$  parameter. The correlation coefficients results  $r = -0.83$  and  $-0.63$ , for  $\alpha$  and  $\beta$  respectively. Figure shows also the linear trend between  $D$  and the coefficients.

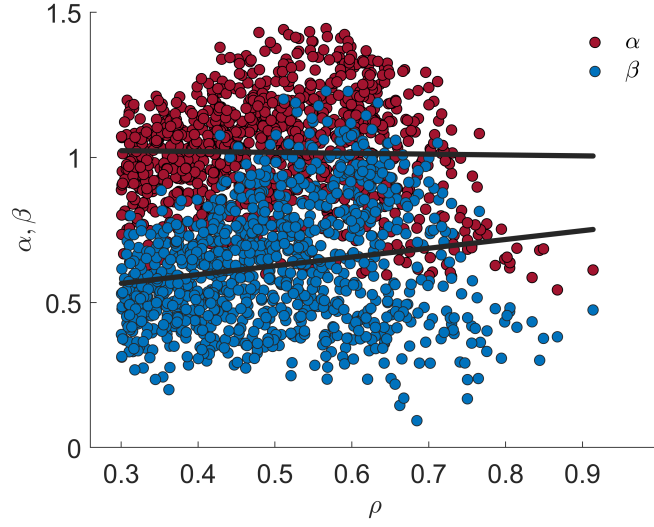


Figure 6: EDFA coefficients  $\alpha$  and  $\beta$  obtained for the simulated COP time series and scattered in relation to  $\rho$  parameter. The correlation coefficients results  $r = -0.019$  and  $0.17$ , for  $\alpha$  and  $\beta$  respectively. Figure shows also the linear trend between  $\rho$  and the coefficients.

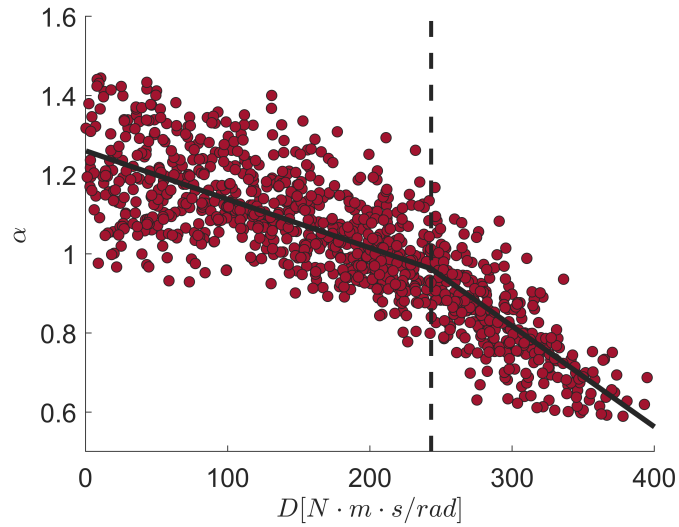


Figure 7: EDFA  $\alpha$  coefficient scattered against  $D$  parameter. The two lines of the best fitting model are reported in black and the knot point is indicated with the dashed, vertical line.

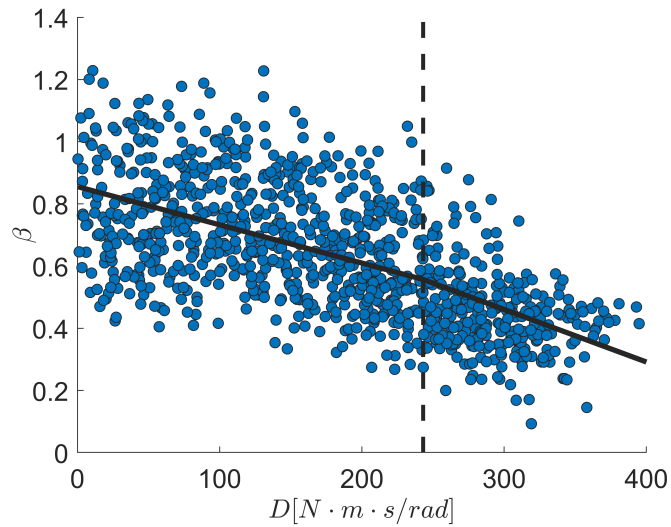


Figure 8: EDFA  $\beta$  coefficient scattered against  $D$  parameter. The two lines of the best fitting model are reported in black and the knot point is indicated with the dashed, vertical line.

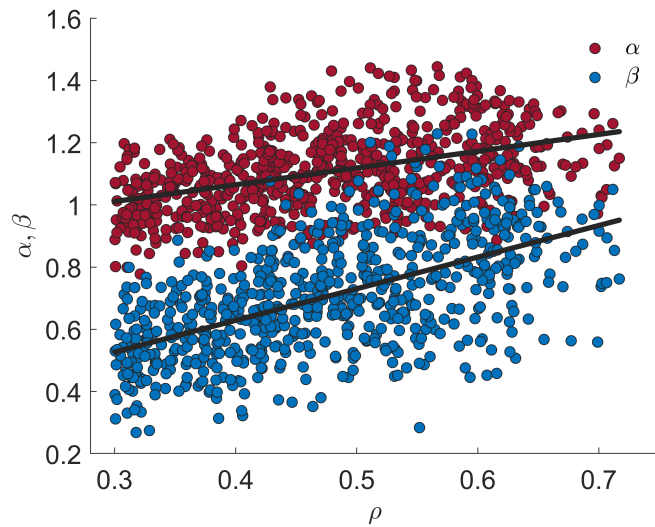


Figure 9: EDFA coefficients  $\alpha$  and  $\beta$  obtained for the simulated COP time series and scattered in relation to  $\rho$  parameter for  $D < 243 N \cdot m \cdot s \cdot rad^{-1}$ . Figure shows also the linear trend between  $\rho$  and the coefficients.

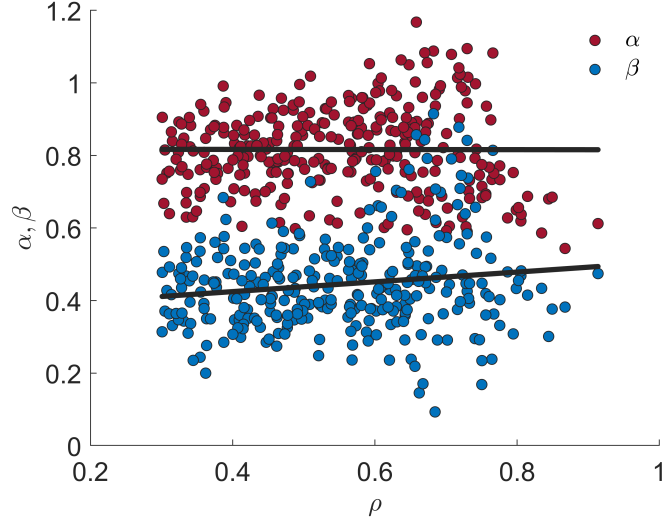


Figure 10: EDFA coefficients  $\alpha$  and  $\beta$  obtained for the simulated COP time series and scattered in relation to  $\rho$  parameter for  $D \geq 243 \text{ N} \cdot \text{m} \cdot \text{s} \cdot \text{rad}^{-1}$ . Figure shows also the linear trend between  $\rho$  and the coefficients.

189 As highlighted in section 2.1, the motor control paradigm examined in this  
 190 study depends upon  $\rho$ ,  $P$ , and  $D$ . The EDFA coefficients showed different  
 191 relationship with the above mentioned parameters when considered over their  
 192 whole range of variation (Table 1). Globally, the  $P$  parameter did not appear  
 193 related to neither the long term correlation properties, nor to the inhomogeneity  
 194 of the simulated COP time-series, as showed by the poor correlation between  
 195  $P$ ,  $\alpha$ , and  $\beta$  (Fig. 4). This confirms that when  $P$  is large enough to compensate  
 196 the portion of the gravitational toppling torque not counteracted by the passive  
 197 muscles properties ( $K$  and  $B$ ), a wide range of values is admissible for  $P$  and  
 198 thus, with respect to  $D$ , its role becomes less crucial for the control model [6, 10].  
 199 The latter aspect aligns with the strong relation observed between both EDFA  
 200 coefficients and  $D$  (Fig. 5), highlighted by the significant correlations of the  
 201 derivative gain with  $\alpha$  and  $\beta$  ( $r = -0.83$  and  $r = -0.63$ ,  $p < 0.0001$ ). In passing,  
 202 the  $\alpha - D$  relation (Fig. 5) points out that the higher is  $D$ , the lower is the  
 203 long-term correlation of the COP timeseries, in agreement with previous studies

204 that reported lower values of  $\alpha$  in elderly populations, where a degraded motor  
205 control can be assumed [19, 29]. This was confirmed also in [7], where it was  
206 observed that patients affected by Parkinson’s disease showed higher  $D$  values  
207 if compared to healthy elderly. Indeed, control schemes with large derivative  
208 gain constitutes an energetically inefficient control strategy, with inflexible and  
209 non-reactive stabilizing mechanism, marked by lower  $\alpha$  values [7].

210 As happened for  $P$ , also  $\rho$  did not show any significant correlation with  $\alpha$   
211 and  $\beta$  coefficients (Fig. 6), indicating that, despite the significant role of  $\rho$   
212 in defining the exchange between the ON and OFF sub-dynamics (see section  
213 2.1), it appears to be not directly related with the stochastic properties of COP  
214 timeseries quantified through the EDFA. In addition, it deserves to be noted  
215 that, within the range of  $P$  and  $D$  values selected in this study (Table 1), stable  
216 simulations were obtained for  $\rho$  up to  $\simeq 0.9$ , although  $\rho$  was free to vary with  
217 the upper bound set to 1 (Table 1). This indicates that the condition for a fully  
218 continuous control ( $\rho = 1$ ) was not reached and thus findings of this study hold  
219 when an intermittent control takes place.

220 For what concerns the  $\beta$  coefficient, it can be observed that the inhomogene-  
221 ity of the COP timeseries decreases for progressively higher values of  $D$  (Fig. 5).  
222 The coefficient  $\beta$  was defined to indicate departure from the power law behavior  
223 (8), since the standard deviation of the profile from the local trend (7) can vary  
224 significantly among the different segments [22]. A reduction of inhomogeneity  
225 implies COP timeseries characterized by regular oscillatory fluctuations, closer  
226 to a stationary behavior. Hence, the  $\beta$  coefficient can provide additive informa-  
227 tion regarding the organization of biological signals in terms of complexity, since  
228 it provides a quantitative measure of local transients [22]. The lower  $\beta$  values  
229 observed for increasing derivative gains appears in agreement also with the *loss*  
230 *of complexity* paradigm [30]. This hypothesis essentially states that healthy  
231 physiological systems produce responses that are complex in the sense of non  
232 linear correlations and long-term dynamics, while a functions’ breakdown, due  
233 to aging or disease, leads to less complex outputs that mirror a reduced ability  
234 in producing an adaptive set of responses when facing motor, cognitive or neu-



235 rological needs [31, 32]. Thus, the reduction of  $\beta$  coefficient highlights a loss of  
 236 fine-structures in COP epochs and it suggests a reduced capability to cope with  
 237 balance demands, relying on a set of few and repeatable postural patterns with  
 238 a limited physiological adaptability. Hence, a lower degree of inhomogeneity  
 239 could reflect a rearrangement in the CNS motor control schemes due to certain  
 240 pathologies, resembling an inefficient tuning of the IP active controller [7, 33].

241 The above mentioned analysis indicates that, among the three ICP,  $D$  gain  
 242 alone reflects changes in the long-term correlation and inhomogeneity properties  
 243 of the whole COP timeseries. This aspect is strengthened also by considering  
 244 separately  $\alpha - D$  and  $\beta - D$  relations (Figs. 7 and 8). In both cases, it appeared  
 245 that the inter-dependence between  $D$  and EDFA coefficients can be fitted with  
 246 two straight lines characterized by different slopes, highlighting the possible  
 247 existence of two different relationships, depending upon  $D$  values. In order to  
 248 test this hypothesis, both the  $\alpha - D$  and  $\beta - D$  were fitted through a least-  
 249 square spline approach [34], testing respectively the existence of three models,  
 250 described by one, two, and three polynomials of order 1. The criterion used  
 251 for assessing the best model was the normalized Akaike's information criterion  
 252 (nAIC) [35], for which the most accurate model presents the lowest nAIC. For  
 253 both  $\alpha - D$  and  $\beta - D$  data distributions, the best fitting model was that with a  
 254 single knot point and thus with two lines: in this case the nAIC resulted equal  
 255 to  $-4.67$  versus  $-4.57$  (one line) and  $-4.40$  (three lines) for  $\alpha - D$ . Similarly,  
 256 for  $\beta - D$  the two-lines model presented a nAIC of  $-3.67$  versus  $-3.60$  (one line)  
 257 and  $-3.52$  (three lines). In addition, in both cases the crossing point between  
 258 the two lines (the knot), presented the same value, i.e.  $D = 243 \text{ N} \cdot \text{m} \cdot \text{s} \cdot \text{rad}^{-1}$   
 259 (Figs. 7 and 8).

260 Given the presence of two different kind of relations between  $D$  and EDFA  
 261 coefficients, a further analysis was performed regarding the correlation between  
 262  $\alpha$  and  $\beta$  with the other two control parameters, i.e.  $P$  and  $\rho$ . Hence, those  $P$  and  
 263  $\rho$  values for which the correspondent  $D$  gain was respectively  $< 243 \text{ N} \cdot \text{m} \cdot \text{s} \cdot \text{rad}^{-1}$   
 264 and  $\geq 243 \text{ N} \cdot \text{m} \cdot \text{s} \cdot \text{rad}^{-1}$  were separately taken into account. To be noted, such  $D$   
 265 value was obtained directly from the above mentioned data-driven analysis and

266 thus it cannot be claimed that it represents a critical value for the intermittent  
267 control scheme. Its possible physical meaning, however, deserves to be carefully  
268 investigated in future studies, also in relation to the other ICP.

269       Regarding the proportional gain, as happened when the  $\alpha - P$  and  $\beta - P$   
270 correlations were examined over the entire range of the proportional gain (Fig.  
271 4), neither  $\alpha$  nor  $\beta$  showed any direct relation with  $P$  ( $r = -0.36$  and  $-0.32$  for  
272  $D < 243 N \cdot m \cdot s \cdot rad^{-1}$  and  $r = -0.19$  and  $-0.11$  for  $D \geq 243 N \cdot m \cdot s \cdot rad^{-1}$ ).  
273 This supports once more that within the range of values assumed by  $P$  in this  
274 study, its variations seem to not consistently affect the COP fractal properties  
275 measured by EDFA.

276       On the other hand, the  $\rho$  parameter showed a different behavior with respect  
277 to  $\alpha$  and  $\beta$  depending upon the values assumed by the derivative gain. When  $D$   
278 is lower than  $243 N \cdot m \cdot s \cdot rad^{-1}$ , both  $\alpha$  and  $\beta$  showed a significant ( $p < 0.0001$ )  
279 correlation with  $\rho$  ( $r = 0.44$  and  $0.61$ , respectively, Fig. 9). This suggests that  
280 the stochastic behavior and the inhomogeneity of a timeseries, quantified by the  
281 EDFA coefficients, manifest a direct relationship with the intermittent nature  
282 of balance control when  $D$  assumes typical values for this control strategy [7].  
283 Incidentally, this is also in agreement with  $\rho$  values that not overcome  $\simeq 0.7$ ,  
284 which permits to exploit the two main features of the intermittent control: the  
285 stable manifold belonging to the OFF-dynamics and the spiraling state steering  
286 induced by the delayed unstable dynamic of the ON-subsystem. This eventually  
287 permits to obtain limit cycle stability without the need of greater control efforts  
288 [7]. In addition, the correlation between  $\alpha$  and two control parameters ( $D$  and  
289  $\rho$ ) aligns with the findings by Yamamoto et al. [28], who reported that the slope  
290 of the COP power spectrum at the LB, which is directly related to  $\alpha$  [36], is a  
291 universal characteristic of postural sway, associated to neural control strategies.  
292 Considering that, despite both trends are significant,  $\beta$  highlights a greater ca-  
293 pability in detecting changes in  $\rho$ , if compared to  $\alpha$ , and thus it further supports  
294 the use of the extended version of the DFA for analyzing posturographic data.

295       Finally, it is interesting to note that the  $\alpha$  coefficient maintains in any case  
296 values quite close to 1 (Fig. 9), possibly referring to an attempt to maintain

297 the output of the balance regularization, i.e. the COP, close to a  $1/f$  process.  
 298 Indeed, the latter is frequently encountered in different physiological time-series,  
 299 characterizing a healthy motor control [27, 37, 38]. On the other hand, the  $\beta$   
 300 coefficient covered a larger set of values (Fig. 9), pointing out that the sim-  
 301 ulated COP timeseries exhibited different degrees of irregularity in their local  
 302 structures [23, 22]. The latter can be associated with the complexity of the  
 303 physiological system generating the data[22], which in healthy conditions is  
 304 commonly characterized by a higher complexity [38, 39], leading in turn to an  
 305 enhanced robustness and adaptability of the response [39, 40].

306 Present results indicate that, when relatively low  $D$  values are used in the  
 307 active controller, the  $\rho$  parameter is connected to the degree of inhomogeneity  
 308 of the COP and thus to the complexity of the balance regulation. This can  
 309 motivate additional studies aimed at investigating how the tuning of the  $S_{on}$  and  
 310  $S_{off}$  regions impacts on the irregularity and complexity of the COP fluctuations.  
 311 It should be noted that the EDFA investigated in this study provides a single-  
 312 scale analysis, accounting for a global description of the data [23, 22], whereas  
 313 many previous studies demonstrated the value of a multi-scale approach for COP  
 314 timeseries [14, 19, 27, 32, 40]. This is also supported by present results, which  
 315 highlighted different dynamics over different temporal scales (Fig. 2). Therefore,  
 316 future works should be devoted to apply EDFA in a multi-scale analysis, in order  
 317 to gain insights regarding the inhomogeneity of COP timeseries over different  
 318 sub-dynamics.

319 When the derivative gain assumes values higher than  $243 N \cdot m \cdot s \cdot rad^{-1}$ , the  
 320  $P$  gain remains unrelated to both  $\alpha$  and  $\beta$ , as highlighted by the poor correlation  
 321 coefficients ( $r = -0.19$  and  $-0.11$ , respectively). In this case the same holds  
 322 also for the  $\rho$  parameter (Fig. 10), for which the correlations observed in the  
 323 previous case completely disappeared ( $r = -0.0021$  for  $\alpha - \rho$  and  $r = -0.14$  for  
 324  $\beta - \rho$ ). A possible explanation for this behavior can be proposed considering  
 325 that, for such range of  $D$  values, the  $S_{on}$  dynamics can stabilize the IP process  
 326 *per se* [7], without the need for switching between sub-dynamics, since with this  
 327 range of  $D$  values ( $\geq 243 N \cdot m \cdot s \cdot rad^{-1}$ ) the  $(P, D)$  of the ON-subsystem is

328 located inside the stability region reported by Suzuki et al. [7]. In this context,  
329 the control policy mimics a stabilizing delayed continuous control [7] and thus it  
330 is reasonable to assume that  $\rho$  becomes less crucial within this control scheme,  
331 losing its relations with EDFA coefficients.

332 Outcomes of this study indicate that the  $\alpha$  and  $\beta$  coefficients introduced by  
333 the EDFA provides additional information on local COP structures, which in  
334 turns are related to the parameters of the intermittent control model. Further,  
335 EDFA resulted able to highlight subtle properties of sway fluctuation data which  
336 can be observed if different ranges of control parameters' values are separately  
337 taken into account. Hence, EDFA can be used together with the classical DFA  
338 exponent to better characterize the upright balance maintenance under the in-  
339 termittent control regime, since inhomogeneity and long term correlations can  
340 be useful descriptors of the hidden postural control paradigm.

#### 341 4. Conclusion

342 In this study, the EDFA was used to investigate the COP time-series gener-  
343 ated by using an IP model, intermittently controlled at the ankle. The IP  
344 model was used to simulate the dynamics of the human balance maintenance in  
345 the anterior-posterior direction [10]. The intermittent motor control paradigm  
346 confirmed to be adequate to simulate COP that presented characteristics of  
347 long-term correlation, as those observed for real data [4]. Moreover, the con-  
348 cept of inhomogeneity introduced in the EDFA turned out to be suitable for  
349 characterizing inner properties of the balance regulation output. The  $\beta$  coeffi-  
350 cient was coupled to the hidden controller parameter  $D$  and  $\rho$ , showing different  
351 relations depending upon the derivative gain values investigated.

352 In addition, the modeling approach here employed resulted useful to high-  
353 light possible interpretation that the EDFA analysis can provide when applied  
354 to real data. Indeed, in a real scenario, functional rearrangements of the CNS  
355 can be identified in changes in the controller parameters, using opportune iden-  
356 tification procedures [33, 7]. Hence, EDFA, embedding the concept of inhom-

357 geneity, can be particularly suitable in posturography to highlight differences in  
358 balance strategies between healthy and pathological groups. Lastly, the choice  
359 of using COP rather than other time series, i.e., COM and joints angles, lies  
360 on an important practical consideration, since COP is directly measurable from  
361 force-plate and it does not require any patient instrumentation or estimation  
362 procedure.

### 363 **References**

- 364 [1] V. Lippi, Prediction in the context of a human-inspired posture control  
365 model, *Robotics and Autonomous Systems* 107 (2018) 63–70.
- 366 [2] T. Mergner, K. Tahboub, Neurorobotics approaches to human and hu-  
367 manoid sensorimotor control., *Journal of physiology, Paris* 103 (3-5) (2009)  
368 115–118.
- 369 [3] J. Błaszczyk, R. Orawiec, D. Duda-Kłodowska, G. Opala, Assessment  
370 of postural instability in patients with parkinson’s disease, *Experimental*  
371 *Brain Research* 183 (1) (2007) 107–114.
- 372 [4] H. Amoud, M. Abadi, D. J. Hewson, V. Michel-Pellegrino, M. Doussot,  
373 J. Duchêne, Fractal time series analysis of postural stability in elderly  
374 and control subjects, *Journal of neuroengineering and rehabilitation* 4 (1)  
375 (2007) 12.
- 376 [5] A. Bottaro, Y. Yasutake, T. Nomura, M. Casadio, P. Morasso, Bounded  
377 stability of the quiet standing posture: an intermittent control model, *Hu-*  
378 *man movement science* 27 (3) (2008) 473–495.
- 379 [6] P. Morasso, A. Cherif, J. Zenzeri, Quiet standing: The single inverted  
380 pendulum model is not so bad after all, *PloS one* 14 (3) (2019) e0213870.
- 381 [7] Y. Suzuki, A. Nakamura, M. Milosevic, K. Nomura, T. Tanahashi, T. Endo,  
382 S. Sakoda, P. Morasso, T. Nomura, Postural instability via a loss of inter-  
383 mittent control in elderly and patients with parkinson’s disease: A model-

- 384 based and data-driven approach, *Chaos: An Interdisciplinary Journal of*  
385 *Nonlinear Science* 30 (11) (2020) 113140.
- 386 [8] I. Schut, J. Pasma, J. Roelofs, V. Weerdesteyn, H. van der Kooij,  
387 A. Schouten, Estimating ankle torque and dynamics of the stabilizing mech-  
388 anism: no need for horizontal ground reaction forces, *Journal of Biomechan-*  
389 *ics* (2020) 109813.
- 390 [9] R. J. Peterka, Sensory integration for human balance control, *Handbook of*  
391 *clinical neurology* 159 (2018) 27–42.
- 392 [10] Y. Asai, Y. Tasaka, K. Nomura, T. Nomura, M. Casadio, P. Morasso, A  
393 model of postural control in quiet standing: robust compensation of delay-  
394 induced instability using intermittent activation of feedback control, *PLoS*  
395 *One* 4 (7) (2009) e6169.
- 396 [11] P. G. Morasso, M. Schieppati, Can muscle stiffness alone stabilize upright  
397 standing?, *Journal of Neurophysiology* 82 (3) (1999) 1622–1626.
- 398 [12] P. G. Morasso, V. Sanguineti, Ankle muscle stiffness alone cannot stabilize  
399 balance during quiet standing, *Journal of neurophysiology* 88 (4) (2002)  
400 2157–2162.
- 401 [13] Y. Suzuki, T. Nomura, M. Casadio, P. Morasso, Intermittent control with  
402 ankle, hip, and mixed strategies during quiet standing: a theoretical pro-  
403 posal based on a double inverted pendulum model, *Journal of Theoretical*  
404 *Biology* 310 (2012) 55–79.
- 405 [14] J. J. Collins, C. J. De Luca, Open-loop and closed-loop control of posture: a  
406 random-walk analysis of center-of-pressure trajectories, *Experimental brain*  
407 *research* 95 (2) (1993) 308–318.
- 408 [15] R. J. Peterka, Postural control model interpretation of stabilogram diffusion  
409 analysis, *Biological cybernetics* 82 (4) (2000) 335–343.

- 410 [16] L. Baratto, P. G. Morasso, C. Re, G. Spada, A new look at posturographic  
411 analysis in the clinical context: sway-density versus other parameterization  
412 techniques, *Motor control* 6 (3) (2002) 246–270.
- 413 [17] P. Morasso, Centre of pressure versus centre of mass stabilization strate-  
414 gies: the tightrope balancing case, *Royal Society open science* 7 (9) (2020)  
415 200111.
- 416 [18] T. E. Prieto, J. B. Myklebust, R. G. Hoffmann, E. G. Lovett, B. M. Myk-  
417 lebust, Measures of postural steadiness: differences between healthy young  
418 and elderly adults, *IEEE Transactions on biomedical engineering* 43 (9)  
419 (1996) 956–966.
- 420 [19] J. Collins, C. De Luca, A. Burrows, L. Lipsitz, Age-related changes in open-  
421 loop and closed-loop postural control mechanisms, *Experimental Brain Re-*  
422 *search* 104 (3) (1995) 480–492.
- 423 [20] V. M. Zatsiorsky, M. Duarte, Rambling and trembling in quiet standing,  
424 *Motor control* 4 (2) (2000) 185–200.
- 425 [21] M. Jacono, M. Casadio, P. G. Morasso, V. Sanguineti, The sway-density  
426 curve and the underlying postural stabilization process, *Motor control* 8 (3)  
427 (2004) 292–311.
- 428 [22] A. N. Pavlov, A. S. Abdurashitov, A. Koronovskii Jr, O. N. Pavlova,  
429 O. Semyachkina-Glushkovskaya, J. Kurths, Detrended fluctuation analy-  
430 sis of cerebrovascular responses to abrupt changes in peripheral arterial  
431 pressure in rats, *Communications in Nonlinear Science and Numerical Sim-*  
432 *ulation* 85 (2020) 105232.
- 433 [23] A. Pavlov, A. Dubrovsky, A. Koronovskii Jr, O. Pavlova, O. Semyachkina-  
434 Glushkovskaya, J. Kurths, Extended detrended fluctuation analysis of elec-  
435 troencephalograms signals during sleep and the opening of the blood–brain  
436 barrier, *Chaos: An Interdisciplinary Journal of Nonlinear Science* 30 (7)  
437 (2020) 073138.

- 438 [24] O. Pavlova, A. Pavlov, Scaling features of intermittent dynamics: Differences  
439 of characterizing correlated and anti-correlated data sets, *Physica A: Statistical Mechanics and its Applications* 536 (2019) 122586.
- 441 [25] D. A. Winter, *Biomechanics and motor control of human gait: normal, elderly and pathological*, 1991.
- 443 [26] C.-K. Peng, S. Havlin, H. E. Stanley, A. L. Goldberger, Quantification  
444 of scaling exponents and crossover phenomena in nonstationary heartbeat  
445 time series, *Chaos: an interdisciplinary journal of nonlinear science* 5 (1)  
446 (1995) 82–87.
- 447 [27] P. Gilfriche, V. Deschodt-Arsac, E. Blons, L. M. Arsac, Frequency-specific  
448 fractal analysis of postural control accounts for control strategies, *Frontiers in physiology* 9 (2018) 293.
- 450 [28] T. Yamamoto, C. E. Smith, Y. Suzuki, K. Kiyono, T. Tanahashi, S. Sakoda,  
451 P. Morasso, T. Nomura, Universal and individual characteristics of postural  
452 sway during quiet standing in healthy young adults, *Physiological reports*  
453 3 (3) (2015) e12329.
- 454 [29] A. Tigrini, F. Verdini, S. Fioretti, A. Mengarelli, Center of pressure plausi-  
455 bility for the double-link human stance model under the intermittent control  
456 paradigm, *Journal of Biomechanics* 128 (2021) 110725.
- 457 [30] L. A. Lipsitz, Dynamics of stability: the physiologic basis of functional  
458 health and frailty, *The Journals of Gerontology Series A: Biological Sciences and Medical Sciences* 57 (3) (2002) B115–B125.
- 460 [31] A. L. Goldberger, C.-K. Peng, L. A. Lipsitz, What is physiologic complexity  
461 and how does it change with aging and disease?, *Neurobiology of Aging*  
462 23 (1) (2002) 23–26.
- 463 [32] M. Costa, A. Priplata, L. Lipsitz, Z. Wu, N. Huang, A. L. Goldberger,  
464 C.-K. Peng, Noise and poise: enhancement of postural complexity in the



- 465 elderly with a stochastic-resonance-based therapy, *EPL (Europhysics Letters)* 77 (6) (2007) 68008.
- 466
- 467 [33] M. L. Corradini, S. Fioretti, T. Leo, R. Piperno, Early recognition of postural disorders in multiple sclerosis through movement analysis: a modeling study, *IEEE Transactions on Biomedical Engineering* 44 (11) (1997) 1029–1038.
- 468
- 469
- 470
- 471 [34] X. Zhang, J. G. Andrews, Downlink cellular network analysis with multi-slope path loss models, *IEEE Transactions on Communications* 63 (5) (2015) 1881–1894.
- 472
- 473
- 474 [35] L. Ljung, *System identification-theory for the user* 2nd edition ptr prentice-hall, 1999.
- 475
- 476 [36] T. Nomura, S. Oshikawa, Y. Suzuki, K. Kiyono, P. Morasso, Modeling human postural sway using an intermittent control and hemodynamic perturbations, *Mathematical Biosciences* 245 (1) (2013) 86–95.
- 477
- 478
- 479 [37] C. Fu, Y. Suzuki, P. Morasso, T. Nomura, Phase resetting and intermittent control at the edge of stability in a simple biped model generates 1/f-like gait cycle variability, *Biological cybernetics* 114 (1) (2020) 95–111.
- 480
- 481
- 482 [38] J. M. Hausdorff, Gait dynamics in parkinson’s disease: common and distinct behavior among stride length, gait variability, and fractal-like scaling, *Chaos: An Interdisciplinary Journal of Nonlinear Science* 19 (2) (2009) 026113.
- 483
- 484
- 485
- 486 [39] S. Thurner, C. Mittermaier, K. Ehrenberger, Change of complexity patterns in human posture during aging, *Audiology and Neurotology* 7 (4) (2002) 240–248.
- 487
- 488
- 489 [40] B. Manor, M. D. Costa, K. Hu, E. Newton, O. Starobinets, H. G. Kang, C. Peng, V. Novak, L. A. Lipsitz, Physiological complexity and system adaptability: evidence from postural control dynamics of older adults, *Journal of Applied Physiology* 109 (6) (2010) 1786–1791.
- 490
- 491
- 492